ACS Catalysis

Letter

pubs.acs.org/acscatalysis

Controlling H^+ vs CO_2 Reduction Selectivity on Pb Electrodes

Chang Hoon Lee and Matthew W. Kanan*

Department of Chemistry, Stanford University, 337 Campus Drive, Stanford, California 94305, United States

Supporting Information

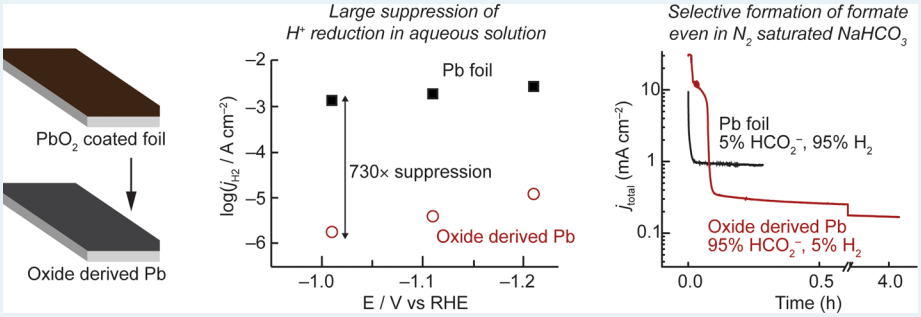

ABSTRACT: Nanocrystalline Pb films prepared by reducing PbO_2 precursors have up to 700-fold lower H^+ reduction activity than polycrystalline Pb foil electrodes but maintain the ability to reduce CO_2. As a result, these "oxide-derived" Pb (OD−Pb) electrodes have higher Faradaic efficiency for CO_2 reduction to HCO_2^- in aqueous solutions with almost no competitive H^+ reduction. Even with very low CO_2 concentrations in N_2-saturated $NaHCO_3$ solution, OD−Pb converts CO_2 derived from HCO_3^- decomposition to HCO_2^- with almost quantitative Faradaic efficiency while Pb foil has less than 10% efficiency. Electrokinetic data suggest that the difference in selectivity between the two electrodes is caused by a difference in the coverage of a surface layer—likely a metastable Pb oxide—that is passivating for H^+ reduction but active for CO_2 reduction.

KEYWORDS: *energy, CO_2, electroreduction, fuel, formate and Pb*

INTRODUCTION

The use of renewable electricity to power the conversion of CO_2 and H_2O into valuable chemicals could reduce net CO_2 emissions.[1−5] The success of this strategy hinges on the development of efficient electroreduction catalysts that selectively and efficiently reduce CO_2 at high rates using H_2O as a H^+ source. One of the fundamental challenges in catalyst development is to suppress H^+ reduction to H_2 without compromising CO_2 reduction. Most materials have a strong preference for H^+ reduction over CO_2 reduction in aqueous electrolytes unless extreme overpotentials are applied, which compromises energetic efficiency.[6]

We have recently explored the use of metal oxides as catalyst precursors and metastable catalytic species to address the challenge of CO_2 versus H^+ reduction selectivity in aqueous electrolytes. In the case of Sn electrodes, we showed that CO_2 reduction requires metastable surface Sn oxides and that enhancing the oxide content of electrodes improves selectivity.[7] For Au and Cu electrodes, oxide layers are not stable under CO_2 reduction conditions. However, Au and Cu electrodes prepared by reducing Au oxide and Cu oxide precursors—"oxide-derived" metals—have very different catalytic properties than bulk materials or nanoparticles.[8−11] Oxide-derived Cu (OD−Cu) and oxide-derived Au (OD−Au) are composed of thin films of interconnected nanocrystallites with 10−100 nm dimensions. In CO_2 reductions, these electrodes have higher selectivity for CO_2 reduction versus H_2 evolution at low overpotential compared to their bulk or nanoparticle counterparts. For OD−Au, this difference is the result of its higher specific (i.e., surface-area-normalized) activity for CO_2 reduction.[9] For OD−Cu, the difference is primarily the result of its lower specific H^+ reduction activity.[8] These studies demonstrate that the microstructure and morphology that result from metal oxide reduction alter the catalytic properties of these metals.

This study examines the factors that control the selectivity for H^+ versus CO_2 reduction on Pb electrodes by comparing Pb foil to oxide-derived Pb (OD−Pb). Several previous studies have evaluated the CO_2 reduction properties of Pb using a variety of different electrode structures, electrochemical cells, and electrolytes.[6] In CO_2-saturated aqueous HCO_3^-, Pb forms primarily HCO_2^- and H_2. The equilibrium potential for the CO_2/HCO_2^- couple in this electrolyte is approximately 0 V versus the reversible hydrogen electrode (RHE; all potentials are reported with respect to this reference).[12] All studies have shown that appreciable CO_2 reduction requires very large overpotentials, but reported results vary widely. Studies with Pb foil electrodes in simple electrochemical H-cells have reported 73%−97% Faraday efficiency (FE) for HCO_2^- at −1.2 V,[6,13] 10% FE at −1.3 V,[14] and 20%−50% at −1.1 to −1.9 V.[15]

Received: November 7, 2014
Revised: December 11, 2014
Published: December 15, 2014

Although some variability is caused by differences in the CO_2 flow rate and HCO_3^- concentration, these results suggest that the reaction is sensitive to subtle features of the Pb surface structure. Interestingly, switching from Pb foil to an electrodeposited Pb electrode improved the FE at −1.1 V from 20% to >90%, although the FE declined over time on the electrodeposited electrode.[15] Experiments with Pb electrodes in gas diffusion cells and liquid flow cells have yielded a range of FEs and current densities that are comparable to the range obtained with Pb foil in H-cells.[16−23]

Here we show that OD−Pb has greatly suppressed H^+ reduction activity compared to polycrystalline Pb foil. This feature leads to improved FE for CO_2 reduction to HCO_2^-, including almost quantitative FE in N_2-saturated HCO_3^- solution with very low CO_2 concentration. The Tafel behavior for H^+ reduction and CO_2 reduction on Pb foil and OD−Pb suggest that the electrodes have different degrees of coverage of a surface layer that is passivating for H_2 evolution but active for CO_2 reduction. This layer is most likely a very thin, metastable Pb^{2+} oxide or hydroxide. The morphology and microstructure of OD−Pb promote a higher coverage of this layer relative to Pb foil.

RESULTS

OD−Pb electrodes were prepared by reducing thick Pb oxide films on polycrystalline Pb foil substrates. The Pb oxide films were grown by long pulsed anodizations in acidic solution (see Supporting Information).[24] X-ray diffraction and X-ray photoelectron spectroscopy (XPS) indicated that the oxide was primarily PbO_2 (Figure S1). The oxidized electrodes were used directly in H_2 evolution or CO_2 reduction electrolyses, during the initial period of which the PbO_2 film was reduced to OD−Pb. Figure 1 shows scanning electron microscopy (SEM), XPS,

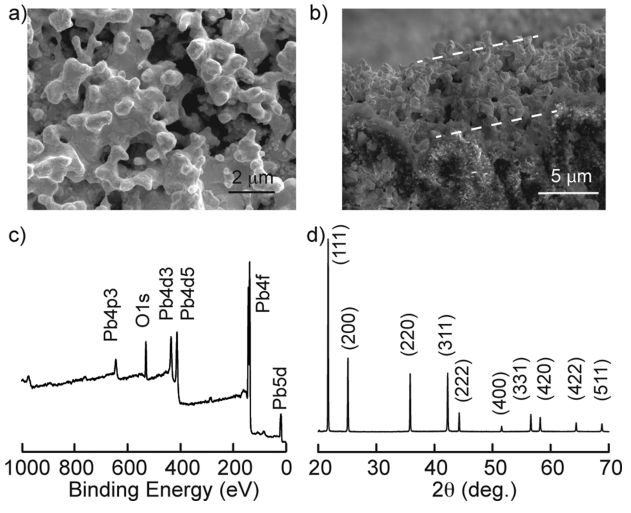

Figure 1. Characterization of oxide-derived Pb (OD−Pb) electrode. (a) Top-down and (b) cross-sectional SEM images. The dashed lines indicate the OD−Pb layer. (c) XPS spectrum. (d) GIXD pattern (11.5 keV).

and grazing incidence X-ray diffraction (GIXD) for a representative OD−Pb electrode after the reduction of the PbO_2 precursor in CO_2-saturated 0.5 M $NaHCO_3$, the electrolyte used for CO_2 reduction (see below). SEM showed that the OD−Pb layer was ∼3 μm thick and composed of aggregated particles with 100−500 nm dimensions. Only peaks associated with Pb^0 were observed by GIXD. Williamson−Hall analysis of the diffraction line shape indicated an average crystallite size of ∼45 nm (Figure S2). High-resolution XPS spectra showed peaks corresponding to Pb^0 and Pb^{2+}. The latter is likely due to the presence of a PbO surface layer, which forms very rapidly on Pb upon brief exposure to air.[25,26] The Pb^{2+} peak was almost completely removed by Ar^+ sputtering (Figure S2), as seen in previous studies of Pb surfaces with a surface oxide. Measurements of the double layer charging currents in 0.5 M $NaClO_4$ indicated that the roughness factor for OD−Pb compared to Pb foil was 25 (Figure S3). Similar roughness factors were obtained for OD−Pb electrodes prepared in different electrolytes.

The H_2 evolution activities of OD−Pb and Pb foil were compared in constant-potential electrolyses performed under N_2 in three different electrolytes: 0.1 M KOH (pH 13), 0.25 M Na_2CO_3 (pH 11.5), and 0.325 M H_2SO_4/$NaHSO_4$ (pH 1.4). OD−Pb was formed from reduction of a thick PbO_2 layer in the electrolyte used for H_2 evolution electrolysis. The steady-state H_2 evolution current densities (j_{H2}) were measured using separate electrolyses or a single stepped-potential electrolysis (see Supporting Information). Figure 2 shows Tafel plots of j_{H2}, including the geometric j_{H2} for both electrodes and the surface-area-normalized j_{H2} for OD−Pb. H_2 evolution was suppressed on OD−Pb relative to Pb foil in all cases. Very large differences were observed in Na_2CO_3 and KOH, where the normalized j_{H2} on OD−Pb was up to ∼730-fold and ∼140-fold lower, respectively. A much smaller suppression was observed under acidic conditions, where normalized j_{H2} was only ∼8-fold lower on OD−Pb. The H_2 Tafel slopes were ∼200 mV dec^{-1} in the acidic electrolyte and >250 mV dec^{-1} in the alkaline electrolytes. The large slopes are likely caused by the presence of a Pb^{2+} surface layer that blocks H^+ reduction (see the Discussion).

To see if the electrolyte in which the PbO_2 precursor is reduced affects the H_2 evolution activity, an OD−Pb electrode was prepared in 0.325 M H_2SO_4/$NaHSO_4$ and then evaluated in 0.25 M Na_2CO_3. The current versus time trace in Na_2CO_3 solution showed a brief initial period of relatively high current before reaching a steady-state value that was very close to the value obtained for an electrode prepared in Na_2CO_3 (Figure S4). The very large suppression of H_2 evolution on OD−Pb in Na_2CO_3 therefore does not require reducing the PbO_2 precursor in this electrolyte.

The CO_2 reduction activities of OD−Pb and polycrystalline Pb were compared in constant-potential electrolyses performed in CO_2-saturated 0.5 M $NaHCO_3$, pH 7.2. The amount of HCO_2^- produced was quantified by NMR analysis of the electrolyte. Gas chromatography of representative electrolyses indicated that H_2 was the only other significant product. Figure 3a shows the FE for HCO_2^- on both electrodes over a range of potentials for which appreciable CO_2 reduction was observed. On OD−Pb, the FE for HCO_2^- was ∼100% from −1.0 to −0.75 V and still ∼90% at −0.70 V. Nearly quantitative FE for HCO_2^- was maintained in a prolonged electrolysis of 75 h at −0.8 V (Figure S5). In contrast, Pb foil exhibited 50% to 60% FE for HCO_2^- from −1.0 to −0.85 V and only 30% at −0.8 V. The Tafel plots of the steady-state current density for HCO_2^- production (j_{HCO2-}) are shown in Figure 3b. When corrected for the difference in surface areas, j_{HCO2-} was similar for OD−Pb and Pb foil from −0.8 to −1.0 V. The origin of the selectivity difference between OD−Pb and Pb foil is therefore the large suppression of H_2 evolution activity on OD−Pb.

dx.doi.org/10.1021/cs5017672 | ACS Catal. 2015, 5, 465−469

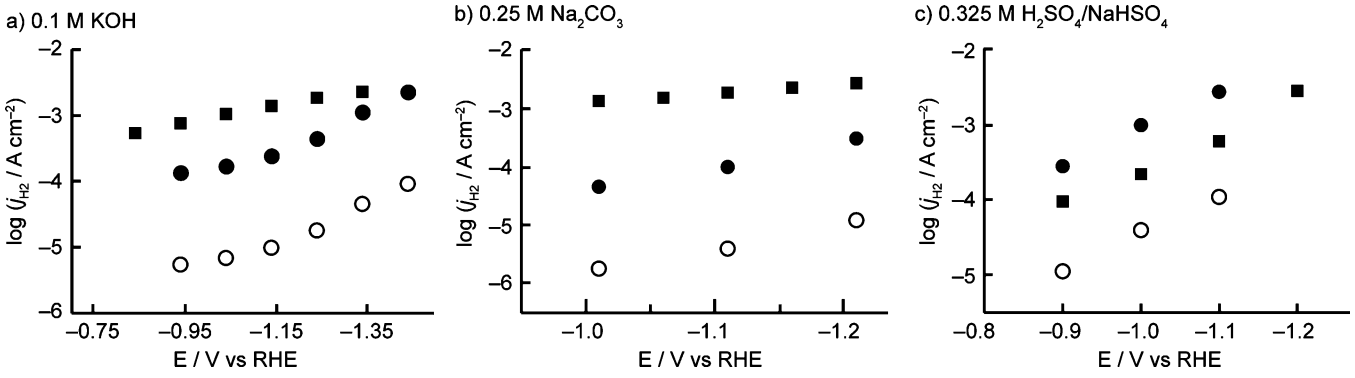

Figure 2. Comparison of the H_2 evolution reaction on Pb foil and OD−Pb. Tafel plots for H_2 evolution in alkaline (a), intermediate (b), and acidic pH (c). Included are the geometric current densities for Pb foil (■) and OD−Pb (●), and the current density for OD−Pb corrected for roughness factor (○).

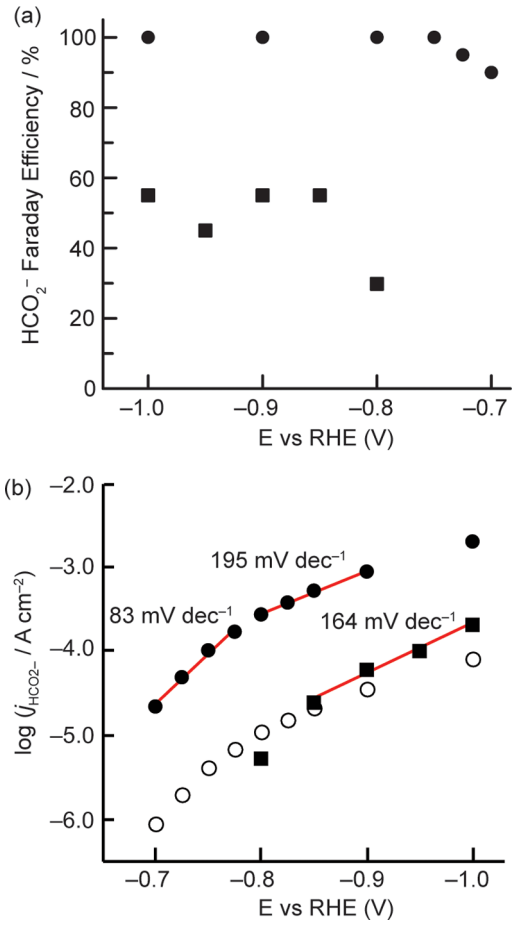

Figure 3. Comparison of CO_2 reduction on Pb foil and OD−Pb in CO_2-saturated 0.5 M $NaHCO_3$. (a) Plot of faradaic efficiency vs potential for Pb foil (■) and OD−Pb (●), (b) Tafel plots of the partial current density for HCO_2^- on Pb foil (■) and OD−Pb (●), and partial current density on OD−Pb corrected for roughness factor (○).

These results demonstrate that it is possible to deactivate the H_2 evolution pathway on Pb while leaving CO_2 reduction unperturbed.

The Tafel slopes in the high overpotential regime were 164 mV dec^{-1} on Pb foil and 195 mV dec^{-1} on OD−Pb (Figure 3b). The reaction was approximately zeroth order in HCO_3^- concentration on OD−Pb at −0.95 V (Figure S6). The Tafel slope decreased to 83 mV dec^{-1} from −0.7 to −0.78 V on OD−Pb, suggesting that there is a different mechanism in this potential range. The relatively low geometric current density for Pb foil precluded reliable measurement of j_{HCO2-} for potentials > −0.8 V.

The selectivity difference between OD−Pb and Pb foil was magnified when electrolysis was performed in N_2-saturated 0.5 M $NaHCO_3$. Although there is very little equilibrium concentration of CO_2 under these conditions, dissociation of HCO_3^- near the electrode surface ($2HCO_3^- \leftrightarrows CO_2 + CO_3^{2-} + H_2O$) supplies enough CO_2 to sustain some CO_2 reduction current density.[27] At −1.0 V in N_2-saturated HCO_3^- solution, OD−Pb still had nearly quantitative FE for HCO_2^- while the FE on Pb foil was <10% (Figure 4). The total geometric

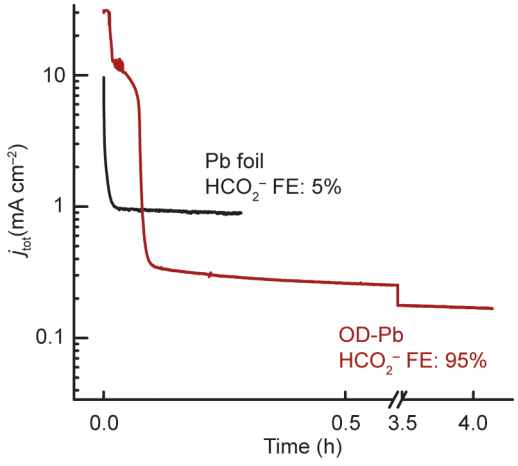

Figure 4. Comparison of CO_2 reduction in N_2-saturated $NaHCO_3$ on Pb foil and OD−Pb. The large initial current for OD−Pb is reduction of the PbO_2 precursor.

current density was significantly higher on Pb foil than OD−Pb despite the higher surface area for the latter. Thus, the suppression of H_2 evolution on OD−Pb enables high selectivity for CO_2 reduction even in electrolytes with low CO_2 concentration.

DISCUSSION

The key functional difference between OD−Pb and Pb foil is the suppression of H_2 evolution on OD−Pb. The Tafel plots provide insight into the origin of this phenomenon. The Tafel slopes for both Pb foil and OD−Pb are very high in KOH and

dx.doi.org/10.1021/cs5017672 | ACS Catal. 2015, 5, 465−469

Na_2CO_3 electrolytes, approaching a regime in which the current density is potential-independent. A previous study of H_2 evolution on Pb foil in H_2SO_4 and NaOH electrolytes also noted a propensity for high Tafel slopes.[28] The slopes were lowered to 120 mV dec^{-1} by using electrolytes that had been pre-electrolyzed for many hours and chemically polishing the Pb surface. The high Tafel slopes on Pb foil and OD−Pb in Figure 2 suggest that the surfaces are mostly passivated for H^+ reduction. Passivation may result from adsorption of electrolyte or impurities, or the presence of a thin film on the surface.

The suppression of H_2 evolution from adsorption of electrolyte impurities would affect Pb foil much more than OD−Pb because of the lower surface area for Pb foil and therefore cannot explain the difference in their activity. We propose that there is a very thin, kinetically stable Pb oxide (hydroxide) layer on the surfaces of the electrodes that blocks H_2 evolution in KOH and Na_2CO_3 electrolytes. H_2 evolution takes place primarily at the remaining exposed Pb^0. The difference in activity between Pb foil and OD−Pb arises from a difference in the coverage of the passivating layer: the oxide covers a large portion (e.g., 90%) of the electrode in the case of Pb foil but an even larger portion (e.g., >99%) in the case of OD−Pb. In acidic electrolyte, the oxide layer is less stable and the coverage is much lower, which results in lower Tafel slopes and a much smaller difference in normalized activity between the two electrodes.

Despite the large difference in their H_2 evolution activity, OD−Pb and Pb foil have similar specific CO_2 reduction activity in HCO_3^- electrolyte. This discrepancy implies that the Pb oxide (hydroxide) layer that passivates the electrodes for H_2 evolution is the active surface for CO_2 reduction. Because the coverage of this layer is high on both Pb foil and OD−Pb, the difference in the coverage between the two electrodes (e.g., 90% vs >99%) has a relatively small effect on the difference in their specific CO_2 reduction activity. In this respect, Pb is similar to Sn, which requires a Sn oxide layer for CO_2 reduction.[7]

The Tafel plots and zeroth order dependence on HCO_3^- for OD−Pb (Figures 3 and S6) are consistent with a CO_2 reduction mechanism in which the rate-determining step is the initial e^- transfer to form a surface-bound $CO_2^{\bullet-}$. Tafel slopes of 120 mV dec^{-1} are more typically observed for rate-limiting e^- transfers, but the surface complexity of Pb under CO_2 reduction conditions could readily account for the higher slopes observed here.

The difference in coverage of a metastable Pb^{2+} layer during catalysis on OD−Pb compared to Pb foil may arise from the relatively high density of defects on OD−Pb. In particular, the grain boundaries between the Pb nanocrystallites in OD−Pb could nucleate Pb^{2+} oxide/hydroxide formation and thereby promote (nearly) full coverage of the electrode surface. This model implies that nanocrystalline or defect-rich Pb electrodes prepared by other methods would also show suppressed H_2 evolution activity, which may explain the transiently improved FE for CO_2 reduction on electrodeposited Pb observed previously.[15] The ability of OD−Pb to maintain selective CO_2 reduction over long electrolyses may reflect greater stability of its morphology and microstructure compared to electrodeposited Pb.

CONCLUSIONS

In summary, OD−Pb has nearly quantitative FE for HCO_2^- in both CO_2- and N_2-saturated HCO_3^- solution at a range of overpotentials where the FE on Pb foil is only 5%−60%. The difference in selectivity arises because the normalized H^+ reduction activity is up to 700-fold lower on OD−Pb, but the intrinsic activity for CO_2 reduction to HCO_2^- is not compromised. Based on the Tafel behavior, both electrodes appear to have a surface layer in alkaline electrolytes that blocks H^+ reduction but catalyzes CO_2 reduction at a low rate. This layer is likely to be a thin, metastable Pb^{2+} oxide or hydroxide. H^+ reduction is suppressed on OD−Pb compared to Pb foil because the coverage of this layer is much higher on OD−Pb as a consequence of its microstructure and morphology.

ASSOCIATED CONTENT

Supporting Information

The following file is available free of charge on the ACS Publications website at DOI: 10.1021/cs5017672.

Experimental procedures and additional data (PDF)

AUTHOR INFORMATION

Corresponding Author

*E-mail: mkanan@stanford.edu.

Notes

The authors declare no competing financial interest.

ACKNOWLEDGMENTS

We thank The Global Climate and Energy Project (award #106765) for support of this work and the Dreyfus Postdoctoral Program in Environmental Chemistry (award #115032) for a fellowship for CHL.

REFERENCES

(1) Peters, M.; Kohler, B.; Kuckshinrichs, W.; Leitner, W.; Markewitz, P.; Muller, T. E. *ChemSusChem* **2011**, *4*, 1216−1240.
(2) Appel, A. M.; Bercaw, J. E.; Bocarsly, A. B.; Dobbek, H.; DuBois, D. L.; Dupuis, M.; Ferry, J. G.; Fujita, E.; Hille, R.; Kenis, P. J. A.; Kerfeld, C. A.; Morris, R. H.; Peden, C. H. F.; Portis, A. R.; Ragsdale, S. W.; Rauchfuss, T. B.; Reek, J. N. H.; Seefeldt, L. C.; Thauer, R. K.; Waldrop, G. L. *Chem. Rev.* **2013**, *113*, 6621−6658.
(3) Aresta, M.; Dibenedetto, A.; Angelini, A. *Chem. Rev.* **2014**, *114*, 1709−1742.
(4) Cole, E. B.; Bocarsly, A. B. In *Carbon Dioxide as Chemical Feedstock*; Aresta, M., Ed.; Wiley-VCH Verlag GmbH & Co. KGaA: Weinheim, Germany, 2010; pp 291−316.
(5) Whipple, D. T.; Kenis, P. J. A. *J. Phys. Chem. Lett.* **2010**, *1*, 3451−3458.
(6) Hori, Y. In *Modern Aspects of Electrochemistry*; Vayenas, C. G., White, R. E., Gamboa-Aldeco, M. E., Eds.; Springer: New York, 2008; Vol. *42*, pp 89−189.
(7) Chen, Y.; Kanan, M. W. *J. Am. Chem. Soc.* **2012**, *134*, 1986−1989.
(8) Li, C. W.; Kanan, M. W. *J. Am. Chem. Soc.* **2012**, *134*, 7231−7234.
(9) Chen, Y.; Li, C. W.; Kanan, M. W. *J. Am. Chem. Soc.* **2012**, *134*, 19969−19972.
(10) Li, C. W.; Ciston, J.; Kanan, M. W. *Nature* **2014**, *508*, 504−507.
(11) Min, X.; Chen, Y.; Kanan, M. W. *Phys. Chem. Chem. Phys.* **2014**, *16*, 13601−13604.
(12) Stalder, C. J.; Chao, S.; Wrighton, M. S. *J. Am. Chem. Soc.* **1984**, *106*, 3673−3675.
(13) Hori, Y. *Chem. Lett.* **1985**, 1695−1698.
(14) Azuma, M.; Hashimoto, K.; Hiramoto, M.; Watanabe, M.; Sakata, T. *J. Electrochem. Soc.* **1990**, *137*, 1772−1778.
(15) Kwon, Y.; Lee, J. *Electrocatalysis* **2010**, *1*, 108.
(16) Köleli, F.; Balun, D. *Appl. Catal., A* **2004**, *274*, 237−242.
(17) Köleli, F.; Atilan, T.; Palamut, N.; Gizir, A. M.; Aydin, R.; Hamann, C. H. *J. Appl. Electrochem.* **2003**, *33*, 447−450.

(18) Innocent, B.; Liaigre, D.; Pasquier, D.; Ropital, F.; Leger, J.-M.; Kokoh, K. B. *J. Appl. Electrochem.* **2009**, *39*, 227−232.
(19) Machunda, R. L.; Lee, J.; Lee, J. *Surf. Interface Anal.* **2010**, *42*, 564−567.
(20) Narayanan, S. R.; Haines, B.; Soler, J.; Valdez, T. I. *J. Electrochem. Soc.* **2011**, *158*, A167−A173.
(21) Alvarez-Guerra, M.; Del Castillo, A.; Irabien, A. *Chem. Eng. Res. Des.* **2014**, *92*, 692−701.
(22) Alvarez-Guerra, M.; Quintanilla, S.; Irabien, A. *Chem. Eng. J.* **2012**, *207*−*208*, 278−284.
(23) Watkins, J. D.; Bocarsly, A. B. *ChemSusChem* **2014**, *7*, 284−290.
(24) Ghasemi, S.; Karami, H.; Mousavi, M. F.; Shamsipur, M. *Electrochem. Commun.* **2005**, *7*, 1257−1264.
(25) Evans, S.; Thomas, J. M. *J. Chem. Soc. Farad. Trans. 2* **1975**, *71*, 313−328.
(26) Farrell, T. *Metal Sci.* **1976**, 87−93.
(27) Hori, Y.; Suzuki, S. *J. Electrochem. Soc.* **1983**, *130*, 2387−2390.
(28) Bockris, J. O. M.; Srinivasan, S. *Electrochim. Act.* **1964**, *9*, 31−44.

dx.doi.org/10.1021/cs5017672 | *ACS Catal.* 2015, 5, 465−469